

Joint Sum-Rate and Power Gain Analysis of an Aerial Base Station

Mohammad Mahdi Azari*, Fernando Rosas†, Kwang-Cheng Chen†, and Sofie Pollin*

* Department of Electrical Engineering, KU Leuven, Belgium

† Graduate Institute of Communication Engineering, National Taiwan University, Taipei, Taiwan

Email: mahdi.azari@kuleuven.be

Abstract—The use of unmanned aerial vehicles (UAVs) as aerial base stations (ABSs) is a promising approach to meet extreme data rate, coverage or power saving requirements in future wireless networks. However, the potential benefits that an ABS can provide depend strongly on its altitude, which affects the fading statistics of its transmissions. In this paper, we propose an altitude dependent performance model that allows to analyze both power and sum-rate capacity gain of the ABS. In contrast to the existing literature, we take into account the height-dependent small-scale fading and path loss exponent in order to provide a complete characterization of the air-to-ground communication links. Our results show that there is an optimal altitude range, representing a trade-off between sum-rate and transmit power gains. Within that optimal range, the height of the ABS can be adapted to optimize for rate or power respectively. The derivations are based on the outage probability of the network, which is studied as function of altitude as well.

Index Terms—Air-to-ground communication, unmanned aerial vehicle (UAV), aerial base station (ABS), outage probability, Rician fading, Marcum Q-function.

I. INTRODUCTION

Aerial communication platforms have been increasingly used to provide wireless services for ground terminals. The quick deployment of unmanned aerial vehicles (UAVs) such as helikites, drones or airships, and their autonomy with respect to terrestrial infrastructure, make them suitable candidates for being deployed in many interesting scenarios. Some examples of this are Facebook Aquila Drone [1] and Google Loon [2], which propose a novel solution for providing internet access from the sky by using the UAVs as aerial base stations (ABSs).

An ABS can be efficiently integrated into cellular wireless networks to either serve the ground users directly or relay traffic to the terrestrial network [3], [4]. In [3], emergency coverage is provided by a UAV to assist the existing terrestrial network. Utilization of a swarm of UAVs is examined in [4] to offload the network traffic from a neighboring cell which is in outage or is overloaded. In the ABSOLUTE project [5], making use of ABSs, a hybrid satellite-UAV-ground network is developed to address public safety and capacity enhancement based on LTE communication systems.

In urban applications the ABS altitude has a strong impact over the network performance. In [6], the authors investigated the optimal placement of a UAV based on simulation, without providing general results or analytical insights in

the various trade-offs. The problem of optimal altitude of the UAV for providing the maximum coverage region is explored in [7]. This work is extended further in [8] by considering two UAVs, a variable transmit power and the impact of interference between UAVs. However, there is no analytic closed-form derivation for the required transmit power and the optimum altitude, giving insight on how the optimum altitude depends on the system parameters. The problem of efficient deployment of multiple UAVs is also investigated in [9] to maximize the coverage area by adjusting the proper altitudes for their locations. It is to be noted that in these interesting works a fixed path loss exponent is considered, which limits the modeling range to high altitudes where the free space assumption is satisfied. Moreover, the effect of multipath and fading and their dependency on UAV's altitude are not considered, which are essential features of the air-to-ground wireless links.

In order to study these problems, a proper model for air-to-ground communication channel is required. With respect to the fading statistics, the Rician model is a natural choice for reflecting the combination of LoS and multipath scatterers, as reported in [10], [11]. In this model the power of fading is determined by the Rician factor, which is highly affected by the ABS elevation angle [12], [13]. In fact, [13] shows that the elevation angle plays a dominant role for determining the Rician factor such that it is larger for higher altitude owing to the presence of less scatters and more probability of LoS. Similarly, as the elevation angle increases the environment between transmitter and receiver becomes less obstructed, which is reflected by a smaller path loss exponent. Although a higher altitude guarantees favorable conditions in terms of fading and path loss exponent, it also generates a larger path loss because of the larger link distance.

The above discussion suggests that there might exist an optimal ABS height at which these effects are balanced. Motivated by this insight, in this paper we study the optimization of the ABS height for maximizing the sum-rate capacity and radiated power gains. For this, we propose a general channel model for air-to-ground wireless links that include height-dependent path loss exponent and fading effects. In contrast to the existent literature [7]–[9], our model is valid also at very low altitudes, which enable us to study the performance gain of an ABS versus a terrestrial base station (TBS).

Our results show that an ABS can provide significant sum-rate and power gains over a TBS. Interestingly, the height that maximizes the sum-rate or minimizes the radiated power are in general not the same, generating a trade-off. Closed-form expressions for the required transmit power and outage probability are derived, which allow to find the optimal height analytically.

The rest of this paper is organized as follows. The system model is presented in Section II. In Section III, the problem statement is defined. The transmit power is analyzed in Section IV and numerical simulations are provided in Section V that confirm our results. Our main conclusions, finally, are presented in Section VI.

II. SYSTEM MODEL

We consider a hybrid air-to-ground communication network with an ABS located at an altitude h , serving a number of ground nodes within its coverage area. The coverage area \mathcal{C} is a disc of radius r_c centered at O , the projection of the ABS on the ground. Without having a prior knowledge regarding the distribution of the ground nodes, we assume that the location of each node follows a two dimensional uniform distribution over \mathcal{C} . A node G is placed at the distance r_G from O and has the elevation angle of $\theta_G = \tan^{-1}(h/r_G)$ with respect to the ABS. As a particular case, when $h = 0$ (and hence $\theta_G = 0$) the system corresponds to a ground-to-ground communication system where the ABS plays the role of a TBS located at O (see Figure 1).

The received SNR at the terminal G , denoted as Γ_G , can be modeled as

$$\Gamma_G = \frac{AP_t}{N_0 \ell_G^\alpha} \Omega_G, \quad (1)$$

where A is a constant containing the impacts of system parameters such as antenna gain and operating frequency, P_t is the transmit power, N_0 is the noise power, α is the path loss exponent, ℓ_G is the distance between the ABS and the terminal G , and $\Omega_G \in [0, \infty)$ is the small-scale fading power which is a variable such that $\bar{\Omega}_G = 1$. Note that the effect of the large-scale path loss is reflected in the path loss exponent, while the small-scale fading effect is included in the distribution of Ω_G .

The Rician distribution can be employed as an appropriate choice to model the small-scale fading between the ABS and the terminal G [10], [11]. Using this model, the fading power Ω_G adopts a non-central chi-squared distribution, whose PDF is given by [14]

$$f_{\Omega_G}(\omega) = \frac{(K+1)e^{-(K+\frac{(K+1)\omega}{\bar{\Omega}_G})}}{\bar{\Omega}_G} I_0\left(2\sqrt{\frac{K(K+1)\omega}{\bar{\Omega}_G}}\right), \quad (2)$$

where $\omega \geq 0$, $I_0(\cdot)$ is the zero order modified Bessel function of the first kind, and $K \in [0, \infty)$ is the Rician factor defined as the ratio between the power of LoS and multipath components. In fact, the larger value of K corresponds to lighter fading where as $K \rightarrow \infty$ the channel converges to

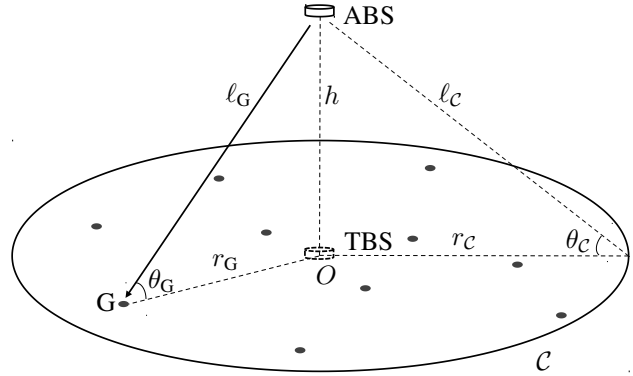


Fig. 1. A typical air-to-ground communication network with a number of ground terminals randomly distributed over the coverage region \mathcal{C} provided by an ABS. A ground node G and the ABS make a communication link with the elevation angle of θ_G .

an AWGN. On the other hand, with $K = 0$ the fading is reduced to a Rayleigh distribution.

Due to the fact that the probability and predominance of the LoS are highly influenced by the elevation angle θ_G [12], [13], the Rician factor is modeled as function of θ_G . Therefore, in order to provide general results that are valid over a wide range of possible scenarios, we consider a general dependency between K and θ_G characterized by the non-decreasing function $K = K(\theta_G)$.

On the other hand, the path loss exponent varies with the elevation angle. In general, the case $\theta_G = 0$ (corresponding to the ground-to-ground link) is the one that endures the largest α , while as θ_G grows α decreases. Therefore, we characterize the path loss exponent as a non-increasing function of θ_G by $\alpha = \alpha(\theta_G)$.

III. PROBLEM FORMULATION

In this section the problem of power and sum-rate gain of an ABS over a TBS is characterized. Our approach is to find the optimal altitudes of the ABS resulting in the maximum gains.

The communication link between the ABS and the terminal G is defined to be in outage when the instantaneous channel SNR falls below a threshold ξ . Thus, the outage probability can be expressed as

$$\mathcal{P}_{out} \triangleq \mathbb{P}(\Gamma_G < \xi), \quad (3)$$

where $\mathbb{P}(E)$ denotes the probability of the event E . Using (1), (2) the outage probability in (3) can be rewritten as

$$\begin{aligned} \mathcal{P}_{out}(r_G, h, P_t) &= \mathbb{P}\left(\frac{AP_t}{N_0 \ell_G^\alpha} \Omega_G < \xi\right) \\ &= 1 - Q\left(\sqrt{2K}, \sqrt{2\xi [1+K] \ell_G^\alpha / \gamma}\right), \end{aligned} \quad (4)$$

where $\ell_G = \sqrt{r_G^2 + h^2}$, $K = K(\theta_G)$, $\alpha = \alpha(\theta_G)$, $\theta_G = \tan^{-1}(h/r_G)$, $Q(\cdot, \cdot)$ is the first order Marcum Q-function, and γ is a shorthand notation for

$$\gamma = \frac{AP_t}{N_0}. \quad (5)$$

The coverage area of an ABS located at an altitude h is a geographical region corresponded to the all locations that satisfy

$$\mathcal{P}_{out}(r_G, h, P_t) \leq \varepsilon, \quad (6)$$

which is a disc centered at O . Above, ε is a target outage performance which represents the minimal tolerable quality of the communication link, which is usually attained at the boundary of the coverage area. At this location, we have

$$\mathcal{P}_{out}(r_C, h, P_t) = \varepsilon. \quad (7)$$

If the target values of r_C and ε are given, the above equation defines a relationship between h and P_t . The value of P_t satisfying this equation is denoted as $P_{t,h}$ and the corresponding γ obtained by replacing $P_t = P_{t,h}$ into (5) is represented by

$$\gamma_h = \frac{AP_{t,h}}{N_0}. \quad (8)$$

Thus, the power gain \mathcal{G}_h^P of an ABS at an altitude h over a TBS ($h = 0$) for covering the same geographical region is defined as

$$\mathcal{G}_h^P \triangleq \frac{P_{t,0}}{P_{t,h}}. \quad (9)$$

The maximum power gain $\hat{\mathcal{G}}_h^P$ is achieved at an optimum altitude \hat{h}_P , where the required transmit power for supporting the region of radius r_C with the target outage performance of ε is minimized.

The average sum-rate of an ABS with the transmit power of P_t is defined as [15]

$$\bar{\mathcal{R}}(h, P_t) = \bar{\mathcal{N}} \cdot W \log_2(1 + \xi)[1 - \bar{\mathcal{P}}_{out}(h, P_t)], \quad (10)$$

where $\bar{\mathcal{N}}$ is the average number of ground nodes within \mathcal{C} , W is the transmission bandwidth, and $\bar{\mathcal{P}}_{out}(h, P_t)$ is the average outage probability $\mathcal{P}_{out}(r_G, h, P_t)$ over the coverage region \mathcal{C} . Note that (10) assumes that all users use a fixed transmission scheme, and hence the data rate for all users that are not in outage is equal to $W \log_2(1 + \xi)$. By denoting the average sum-rate corresponding to $P_t = P_{t,h}$ by $\bar{\mathcal{R}}_h$, one can define the average sum-rate gain \mathcal{G}_h^R provided by an ABS over \mathcal{C} in comparison with a TBS as

$$\mathcal{G}_h^R \triangleq \frac{\bar{\mathcal{R}}_h}{\bar{\mathcal{R}}_0} = \frac{1 - \bar{\mathcal{P}}_{out}(h, P_{t,h})}{1 - \bar{\mathcal{P}}_{out}(0, P_{t,0})}. \quad (11)$$

The altitude which results in the maximum sum-rate gain is denoted as $h = \hat{h}_R$. Interestingly, the above formulation allows us to think that the optimal height at which the sum-rate is maximized might not coincide with the optimal height that minimizes the required radiated power. This issue is studied in the next sections.

IV. POWER ANALYSIS

In this section we derive the required transmit power of an ABS which covers a given region \mathcal{C} . Then the results are used to compute the optimum elevation angle and altitude, and the power and sum-rate gains of the ABS. To this end, first we propose the following theorem.

Theorem 1. *The required transmit power of an ABS in order to cover the geographical region \mathcal{C} is obtained as*

$$P_{t,h} = \frac{N_0}{A} \xi \frac{x_\theta^2 + 2}{y_\theta^2} \left[\frac{r_C}{\cos(\theta_C)} \right]^{\alpha(\theta_C)}, \quad (12)$$

where

$$x_\theta = \sqrt{2K(\theta_C)}, \quad (13a)$$

$$y_\theta = Q^{-1}(x_\theta, 1 - \varepsilon), \quad (13b)$$

$$\theta_C = \tan^{-1}(h/r_C). \quad (13c)$$

Above, $Q^{-1}(\cdot, \cdot)$ is the inverse Marcum Q-function with respect to its first argument and r_C is the radius of \mathcal{C} .

Proof. Using (4) and (7) one can write

$$Q\left(\sqrt{2K(\theta_G)}, \sqrt{2\xi [1 + K(\theta_G)] \ell_G^{\alpha(\theta_G)} / \gamma_h}\right) = 1 - \varepsilon, \quad (14)$$

for $\ell_G = \ell_C$ and $\theta_G = \theta_C$. Thus, by defining an auxiliary variable as

$$x_\theta = \sqrt{2K(\theta_C)}, \quad (15)$$

the equation in (14) is equivalent to

$$\sqrt{2\xi [1 + K(\theta_C)] \ell_C^{\alpha(\theta_C)} / \gamma_h} = y_\theta, \quad (16)$$

where y_θ is the inverse Marcum Q-function in (14) with respect to x_θ , i.e.

$$y_\theta = Q^{-1}(x_\theta, 1 - \varepsilon), \quad (17)$$

and $\ell_C = r_C / \cos(\theta_C)$. Therefore, using (15) and (16) one obtains

$$\gamma_h = \xi \frac{x_\theta^2 + 2}{y_\theta^2} \left[\frac{r_C}{\cos(\theta_C)} \right]^{\alpha(\theta_C)}, \quad (18)$$

and hence (8) and (18) yields

$$P_{t,h} = \frac{N_0}{A} \xi \frac{x_\theta^2 + 2}{y_\theta^2} \left[\frac{r_C}{\cos(\theta_C)} \right]^{\alpha(\theta_C)}. \quad (19)$$

□

Now we can find the power gain as follows.

Corollary 1. *The power gain \mathcal{G}_h^P of an ABS over a TBS can be written as*

$$\mathcal{G}_h^P = \frac{x_0^2 + 2}{y_0^2} \frac{y_\theta^2}{x_\theta^2 + 2} r_C^{\alpha(0) - \alpha(\theta_C)} [\cos(\theta_C)]^{\alpha(\theta_C)}. \quad (20)$$

Proof. Using (9) and (12) the desired result is obtained. □

Notice that for a given $P_{t,0}$ or equivalently γ_0 , the coverage radius r_C can be determined from (18) as

$$r_C = \sqrt[\alpha(\theta_C)]{\frac{\gamma_0 y_0^2}{\xi (x_0^2 + 2)}}, \quad (21)$$

and hence (12) and (20) can be respectively rewritten in terms of γ_0 as

$$P_{t,h} = \frac{N_0}{A} \xi^{1 - \frac{\alpha(\theta_C)}{\alpha(0)}} \left(\frac{\gamma_0 y_0^2}{x_0^2 + 2} \right)^{\frac{\alpha(\theta_C)}{\alpha(0)}} \frac{x_\theta^2 + 2}{y_\theta^2} \left[\frac{1}{\cos(\theta_C)} \right]^{\alpha(\theta_C)},$$

$$\mathcal{G}_h^P = \left(\frac{\gamma_0}{\xi} \right)^{1 - \frac{\alpha(\theta_C)}{\alpha(0)}} \left(\frac{x_0^2 + 2}{y_0^2} \right)^{\frac{\alpha(\theta_C)}{\alpha(0)}} \frac{y_\theta^2}{x_\theta^2 + 2} [\cos(\theta_C)]^{\alpha(\theta_C)}.$$

Moreover, the sum-rate gain \mathcal{G}_h^R can be computed by replacing the transmit power from (12) into (11).

In order to find the power-optimum altitude \hat{h}_P , from the following theorem we find the optimum elevation angle $\hat{\theta}_C$ at which the transmit power $P_{t,h}$ is minimized or equivalently the power gain \mathcal{G}_h^P is maximized.

Theorem 2. *The optimum elevation angle $\hat{\theta}_C$ for achieving the maximum power gain is approximately obtained by solving*

$$\frac{2\eta_\varepsilon}{x_\theta(x_\theta + \eta_\varepsilon)} \cdot x'_\theta + \alpha(\theta_C) \cdot \tan(\theta_C) + \ln \left[\frac{r_C}{\cos(\theta_C)} \right] \cdot \alpha'(\theta_C) = 0, \quad (23)$$

where x'_θ and $\alpha'(\theta_C)$ indicate the derivative functions.

Proof. The proof can be found in Appendix. \square

Notice that \hat{h}_P is obtained by replacing $\theta_C = \hat{\theta}_C$ into (13c).

V. CASE STUDY:

SPECIFIC DEPENDENCY OF K AND α OVER θ_G

In this section we illustrate the capabilities of our model by instantiating it with specific functional dependencies for K and α . In the sequel, in Section V-A the models for the Rician factor and the path loss exponent are presented and then the numerical results are provided in Section V-B.

A. Models for K and α

We assume an exponential dependency between the Rician factor and the elevation angle expressed as

$$K(\theta_G) = a_1 \cdot e^{a_2 \theta_G}, \quad (24)$$

where a_1 and a_2 are determined by the type of environment and the system parameters such as carrier frequency. An exponential dependency is supported by empirical data [13]. Note that a_1 and a_2 are related to $\kappa_0 = K(0)$ and $\kappa_{\frac{\pi}{2}} = K(\frac{\pi}{2})$ by

$$\begin{aligned} a_1 &= \kappa_0 \\ a_2 &= \frac{2}{\pi} \ln \left(\frac{\kappa_{\frac{\pi}{2}}}{\kappa_0} \right). \end{aligned} \quad (25)$$

The dependency between α and θ_G can be studied using the notion of probability of LoS \mathcal{P}_{LoS} between the ABS and ground nodes [7]. This dependency is defined as

$$\alpha(\theta_G) = b_1 \cdot \mathcal{P}_{\text{LoS}}(\theta_G) + b_2, \quad (26)$$

where

$$\mathcal{P}_{\text{LoS}}(\theta_G) = \frac{1}{1 + c_1 e^{-c_2 \theta_G}}, \quad (27)$$

and b_1 , b_2 , c_1 and c_2 are environment and frequency dependent constant parameters. Since $\mathcal{P}_{\text{LoS}}(0) \rightarrow 0$ and

$\mathcal{P}_{\text{LoS}}(\pi/2) \rightarrow 1$, b_1 and b_2 are determined by $\alpha_0 = \alpha(0)$ and $\alpha_{\frac{\pi}{2}} = \alpha(\frac{\pi}{2})$ as

$$\begin{aligned} b_1 &= \alpha_{\frac{\pi}{2}} - \alpha_0, \\ b_2 &= \alpha_0. \end{aligned} \quad (28)$$

Under these assumptions, Theorem 2 provides the following corollary for the optimum elevation angle at the edge of \mathcal{C} , i.e. $\hat{\theta}_C$.

Corollary 2. *Considering (24) and (26), $\hat{\theta}_C$ satisfies the following equation*

$$\begin{aligned} \frac{a_2 \eta_\varepsilon (1 + c_1 e^{-c_2 \theta_C})}{\eta_\varepsilon + \sqrt{2a_1} e^{\frac{a_2 \theta_C}{2}}} + (b_1 + b_2 + b_2 c_1 e^{-c_2 \theta_C}) \tan(\theta_C) \\ + \frac{b_1 c_1 c_2 e^{-c_2 \theta_C}}{1 + c_1 e^{-c_2 \theta_C}} \ln \left[\frac{r_C}{\cos(\theta_C)} \right] = 0. \end{aligned} \quad (29)$$

Proof. Using (26) and (27) and taking derivative of $\alpha(\theta_C)$ yields

$$\alpha'(\theta_C) = \frac{b_1 c_1 c_2 e^{-c_2 \theta_C}}{(1 + c_1 e^{-c_2 \theta_C})^2}. \quad (30)$$

On the other hand, from (15) and (24) we have

$$x'_\theta = \sqrt{\frac{a_1}{2}} a_2 e^{\frac{a_2 \theta_C}{2}}. \quad (31)$$

Therefore, by using (15), (23), (24), (26), (27), (30) and (31) the desired result is attained. \square

B. Numerical Simulations

We provide the numerical results by assuming $\xi = 5$ dB, $\kappa_0 = 5$ dB, $\kappa_{\frac{\pi}{2}} = 15$ dB, $\alpha_0 = 3$, $\alpha_{\frac{\pi}{2}} = 2$, and $(c_1, c_2) = (44, 9)$ [7], unless otherwise is mentioned.

The existence of an optimum θ_C , i.e. $\hat{\theta}_C$, can be seen from the Figure 2 where γ_h is computed using Equation (18) from Theorem 1 for $r_C = 1000$ m. In Table I the exact values of $\hat{\theta}_C$ obtained from the figure are compared with the approximate values calculated from (23), which shows the accuracy of Theorem 2. Note that the slight differences between the exact and approximate values are caused by the proposed approximate solution of $y_\theta = Q^{-1}(x_\theta, 1 - \varepsilon)$ used in the proof of Theorem 2. Figure 2 also illustrates that the required γ_h and hence power $P_{t,h}$ for lower ε is higher such that it is more susceptible to ε at low angles and consequently at low altitudes.

TABLE I. The optimum elevation angle $\hat{\theta}_C$.

ε	$\hat{\theta}_C$ from Figure 2 exact value	$\hat{\theta}_C$ from Theorem 2 approximate value
0.01	49.7°	50°
0.1	47.0°	46.7°
0.5	45.5°	45.5°

The impact of altitude on the power gain is illustrated in Figure 3a. This figure shows that at low altitudes more power gain is achieved for smaller coverage radius r_C , however for high altitudes the power gain is bigger for larger r_C .

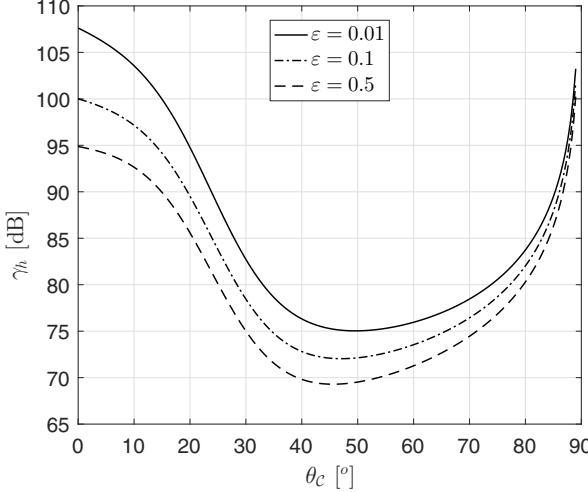


Fig. 2. Simulations confirm that there exist a unique elevation angle at which the required γ_h , and hence transmit power $P_{t,h}$ for guaranteeing a target outage probability, is minimized. Simulations show that the optimal elevation angle increases when the target outage probability is decreased.

These facts finally lead to an increase in the maximum power gain $\hat{\mathcal{G}}_h^P$ for larger r_c . Indeed, $\hat{\theta}_c$ is approximately the same and equal to 45° for all three cases due to the negligible value of $\alpha'(\hat{\theta}_c)$ which eliminates the contribution of r_c for determining $\hat{\theta}_c$ in (23) (The path loss exponent $\alpha(\hat{\theta}_c)$ becomes stable and close to $\alpha_{\frac{\pi}{2}}$ at which the maximum power gain is attained). Therefore, using (20) and due to the constant value of $\hat{\theta}_c$ for different r_c one can write

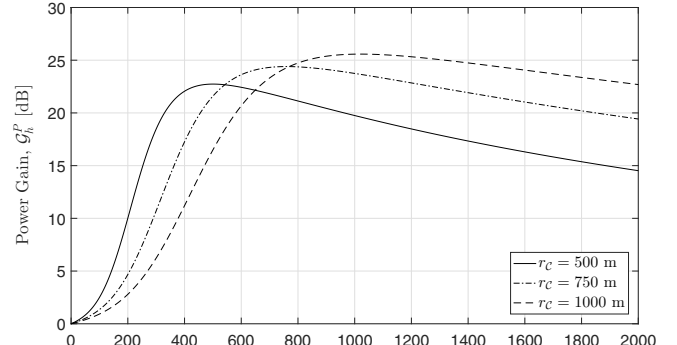
$$\hat{\mathcal{G}}_h^P \propto r_c^{\alpha(0)-\alpha(\hat{\theta}_c)}. \quad (32)$$

As $\hat{\theta}_c$ remains constant, using (13c) the optimum altitude \hat{h}_P becomes proportional to r_c where $\hat{h}_P \cong r_c$ in Figure 3a.

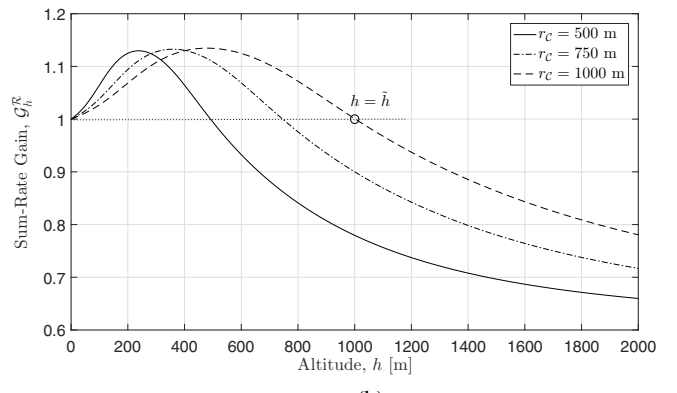
Figure 3b depicts the sum-rate gain expressed in (11) for the same values of system parameters as Figure 3a. As can be seen, although $P_{t,h}$ is lower than $P_{t,0}$ the average sum-rate provided by the ABS is bigger than TBS up to some altitude denoted as \tilde{h} . Interestingly, even at $h = \hat{h}_P$ where $P_{t,h}$ is minimum (see Figure 3a) $\bar{\mathcal{R}}(\hat{h}_P, \hat{P}_{t,h})$ is not degraded compared to $\bar{\mathcal{R}}(0, P_{t,0})$. This figure also shows that \hat{h}_R , where $\bar{\mathcal{R}}(h, P_{t,h})$ is maximized, is different with \hat{h}_P and approximately is equal to $\tilde{h}/2$. Therefore, depending on what is more important a system designer can choose the appropriate altitude for positioning the UAV. Furthermore, from the figure one can see that the sum-rate gain degrades with the size of coverage area at low altitudes whereas at higher altitudes it is higher for larger coverage radius.

VI. CONCLUSION

The power and sum-rate gains of an ABS versus a TBS were analyzed. To this end, we proposed a generic channel model to include the height-dependent small-scale fading and path loss exponent. Using this model, the optimum altitudes at which the power and sum-rate gains are maximized,



(a)



(b)

Fig. 3. Achievable power and sum-rate gains by an ABS with respect to a TBS. Interestingly, the optimal heights for the two cases, i.e. \hat{h}_P and \hat{h}_R , in general do not coincide. Is to be noted that the sum-rate gains are achieved using less transmit power compared to the TBS, as explained in Section III.

were studied. Our results show that using a favorable altitude can bring great capacity and power gains to the system with respect to what a TBS can provide. However, we found that in general the height that maximizes the capacity is not the same as the one that minimizes the power. This introduces a novel trade-off for ABS, which will be studied as part of our future work.

APPENDIX PROOF OF THEOREM 2

In order to find the optimum elevation angle $\hat{\theta}_c$ at which the transmit power $P_{t,h}$ is minimized or equivalently the power gain $\hat{\mathcal{G}}_h^P$ is maximized, we compute the derivative of $P_{t,h}$ with respect to θ_c . To this end, first we propose an approximate solution for the inverse Marcum Q-function to find a simplified relationship between y_θ and x_θ from (13b).

From [16] one sees that

$$\frac{\partial}{\partial y} Q(x, y) = -y e^{-\frac{x^2+y^2}{2}} I_0(xy) < 0, \quad (33)$$

where $I_0(\cdot)$ is the zero-order modified Bessel function of the first kind which returns positive real numbers. Thus, Marcum Q-function $Q(x, y)$ is a strictly decreasing function of its

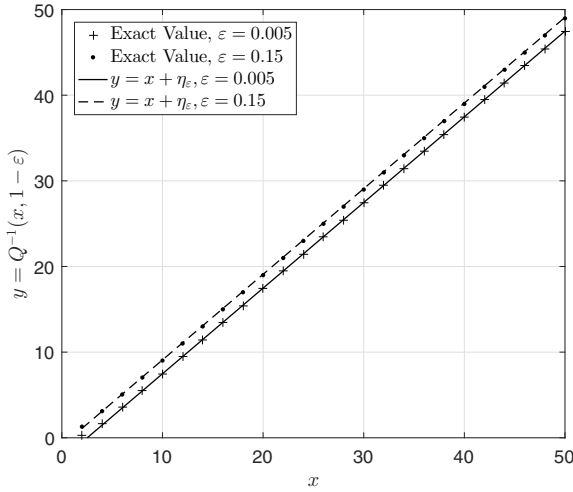


Fig. 4. The analytic approximate solution of $y = Q^{-1}(x, 1 - \varepsilon)$ is in a good conformity with the exact values.

second argument y and hence $Q^{-1}(x, 1 - \varepsilon) = y$ should be an strictly increasing function of $\varepsilon = 1 - Q(x, y)$.

The exact solutions of $y = Q^{-1}(x, 1 - \varepsilon)$ for $\varepsilon = \varepsilon_{\min}, \varepsilon_{\max}$ with $\varepsilon_{\min} \rightarrow 0$ and $\varepsilon_{\max} = 1$ are fitted to the linear curves $y = x - 4.765$ and $y = x + 5.158$ respectively. Therefore, one can write

$$\begin{aligned} Q^{-1}(x, 1 - \varepsilon_{\min}) &= x - 4.765 + \delta_1(x, 1 - \varepsilon_{\min}), \\ Q^{-1}(x, 1 - \varepsilon_{\max}) &= x + 5.158 + \delta_2(x, 1 - \varepsilon_{\max}), \end{aligned} \quad (34)$$

where $\delta_1(x, 1 - \varepsilon_{\min})$ and $\delta_2(x, 1 - \varepsilon_{\max})$ are negligible. For an arbitrary $\varepsilon \in [\varepsilon_{\min}, \varepsilon_{\max}]$ we have

$$Q^{-1}(x, 1 - \varepsilon_{\min}) < Q^{-1}(x, 1 - \varepsilon) < Q^{-1}(x, 1 - \varepsilon_{\max}). \quad (35)$$

Using (34) and (35) for $y = Q^{-1}(x, 1 - \varepsilon)$ one obtains

$$x - 4.765 + \delta_1(x, 1 - \varepsilon_{\min}) < y < x + 5.158 + \delta_2(x, 1 - \varepsilon_{\max}), \quad (36)$$

which proposes the following equation

$$y = x + \eta_\varepsilon + \delta(x, 1 - \varepsilon), \quad (37)$$

where $\delta(x, 1 - \varepsilon)$ is negligible. The value of η_ε can be interpolated using the samples of $\varepsilon = 0.001, 0.01, 0.1, 0.2, 0.3, 0.4$ where $\eta_\varepsilon = -2.937, -2.219, -1.206, -0.772, -0.458, -0.190$ respectively. Using the samples, a quadratic polynomial function of $\ln(\varepsilon)$ for η_ε is obtained which is $\eta_\varepsilon = 0.045[\ln(\varepsilon)]^2 + 0.799\ln(\varepsilon) + 0.443$. Therefore, by replacing η_ε into (37), we finally have

$$y \cong x + \eta_\varepsilon; \quad \eta_\varepsilon = 0.045[\ln(\varepsilon)]^2 + 0.799\ln(\varepsilon) + 0.443. \quad (38)$$

Figure 4 compares the analytic approximate solution of $y = Q^{-1}(x, 1 - \varepsilon)$ in (38) with the exact values, which shows the accuracy of the proposed solution.

Now we take the derivative of $\ln(P_{t,h})$ in (12) with respect to θ_C as follows,

$$0 = \frac{\partial}{\partial \theta_C} \ln(P_{t,h}). \quad (39)$$

Assuming that $x_\theta \gg \sqrt{2}$ for the minimum transmit power, (12) can be simplified to

$$P_{t,h} = \frac{N_0 \xi}{A} \left[\frac{x_\theta}{y_\theta} \right]^2 \left[\frac{r_C}{\cos(\theta_C)} \right]^{\alpha(\theta_C)}. \quad (40)$$

Replacing (40) into (39) yields

$$\begin{aligned} 0 &= \frac{\partial}{\partial \theta_C} \left[\ln \left(\frac{N_0 \xi}{A} \right) + 2 \ln \left[\frac{x_\theta}{y_\theta} \right] + \alpha(\theta_C) \ln \left[\frac{r_C}{\cos(\theta_C)} \right] \right] \\ &= 2 \left[\frac{x'_\theta}{x_\theta} - \frac{y'_\theta}{y_\theta} \right] + \alpha'(\theta_C) \ln \left[\frac{r_C}{\cos(\theta_C)} \right] + \alpha(\theta_C) \tan(\theta_C) \\ &= \frac{2\eta_\varepsilon x'_\theta}{x_\theta(x_\theta + \eta_\varepsilon)} + \ln \left[\frac{r_C}{\cos(\theta_C)} \right] \alpha'(\theta_C) + \alpha(\theta_C) \tan(\theta_C), \end{aligned} \quad (41)$$

where (38) is used in the last equation, and x'_θ, y'_θ and $\alpha'(\theta_C)$ indicate the derivative functions.

REFERENCES

- [1] Facebook, *Connecting the World from the Sky*. Facebook, Technical Report, 2014.
- [2] S. Katikala, "Google project loon," *InSight: Rivier Academic Journal*, vol. 10, no. 2, 2014.
- [3] W. Guo, C. Devine, and S. Wang, "Performance analysis of micro unmanned airborne communication relays for cellular networks," in *Communication Systems, Networks & Digital Signal Processing (CSNDSP), 2014 9th International Symposium on*. IEEE, 2014, pp. 658–663.
- [4] S. Rohde and C. Wietfeld, "Interference aware positioning of aerial relays for cell overload and outage compensation," in *Vehicular Technology Conference (VTC Fall)*. IEEE, 2012, pp. 1–5.
- [5] ABSOLUTE (*Aerial Base Stations with Opportunistic Links for Unexpected and Temporary Events*). <http://www.absolute-project.eu>.
- [6] J. Kosmerl and A. Vilhar, "Base stations placement optimization in wireless networks for emergency communications," in *Communications Workshops (ICC), 2014 IEEE International Conference on*. IEEE, 2014, pp. 200–205.
- [7] A. Al-Hourani, S. Kandeepan, and S. Lardner, "Optimal lap altitude for maximum coverage," *Wireless Communications Letters, IEEE*, vol. 3, no. 6, pp. 569–572, 2014.
- [8] M. Mozaffari, W. Saad, M. Bennis, and M. Debbah, "Drone small cells in the clouds: Design, deployment and performance analysis," *arXiv preprint arXiv:1509.01655*, 2015.
- [9] ———, "Efficient deployment of multiple unmanned aerial vehicles for optimal wireless coverage," *arXiv preprint arXiv:1606.01962*, 2016.
- [10] S. Kandeepan, K. Gomez, L. Reynaud, and T. Rasheed, "Aerial-terrestrial communications: terrestrial cooperation and energy-efficient transmissions to aerial base stations," *Aerospace and Electronic Systems, IEEE Transactions on*, vol. 50, no. 4, pp. 2715–2735, 2014.
- [11] D. W. Matolak, "Air-ground channels & models: Comprehensive review and considerations for unmanned aircraft systems," in *Aerospace Conference, 2012 IEEE*, 2012, pp. 1–17.
- [12] J. Hagenauer, F. Dolainsky, E. Lutz, W. Papke, and R. Schweikert, "The maritime satellite communication channel-channel model, performance of modulation and coding," *Selected Areas in Communications, IEEE Journal on*, vol. 5, no. 4, pp. 701–713, 1987.
- [13] S. Shimamoto *et al.*, "Channel characterization and performance evaluation of mobile communication employing stratospheric platforms," *IEICE transactions on communications*, vol. 89, no. 3, pp. 937–944, 2006.
- [14] M. K. Simon and M.-S. Alouini, *Digital communication over fading channels*. John Wiley & Sons, 2005, vol. 95.
- [15] S. Shalmashi, E. Björnson, M. Kountouris, K. W. Sung, and M. Debbah, "Energy efficiency and sum rate tradeoffs for massive mimo systems with underlaid device-to-device communications," *arXiv preprint arXiv:1506.00598*, 2015.
- [16] R. T. Short, "Computation of rice and noncentral chi-squared probabilities," 2012.